Division of Cardiology, Nanjing First Hospital, Nanjing Medical University

Ginkgolide A protects adverse cardiac remodeling through enhancing antioxidation and nitric oxide utilization in mice with pressure overload

WEI YOU, ZHIMING WU, FEI YE*, XIANGQI WU*

In this study, we aimed to explore whether ginkgolide A (GA) would exhibit cardio-protective effects in mice with pressure overload through enhancing antioxidation and nitric oxide (NO) bioavailability. 21 male mice were randomly assigned into three groups as follows: sham group (10 ml/kg/day PBS, n=7), transverse aortic constriction (TAC) group (TAC and 10 ml/kg/day PBS, n=7) and GA group (TAC and 20 mg/kg/day GA, n=7). All groups received an intraperitoneal injection for four weeks. Heart and body mass were measured. Cardiac function was assessed by echocardiography. The collagen deposition, area of cardiomyocytes, number of capillaries and cell apoptosis were evaluated using Masson's staining, WGA staining, CD31 staining and TUNEL assay, respectively. Cadiac oxidative and antioxidative indexes were measured by colorimetry. Nitrotyrosine (NT) and transforming growth factor-β (TGF-β) were determined by ELISA. Phospho-endothelial NO synthases (eNOS) (Ser1177), phospho-eNOS (Thr 495), eNOS, neuronal NOS (nNOS), inducible NOS (iNOS) and GAPDH were analyzed by western blot. GA treatment greatly improved cardiac dysfunction, suppressed cardiac hypertrophy and increased capillary number at 4 weeks after TAC (P<0.05). Fibrotic area, cardiomyocyte area, and cell apoptosis of GA group were declined notably as compared to those of TAC group (P<0.05). GA administration substantially attenuated cardiac oxidative stress, and reduced NT and TGF-β levels (P<0.05). Besides, GA medication can enhance eNOS signaling, resulting in increased cardiac NO production (P<0.05). GA had a cardioprotective effect in mice with pressure overload, which was closely related with reducing oxidative stress and enhancing NO bioavailability in hearts.

1. Introduction

Chronic heart failure (CHF) is a leading cause of death with an estimated prevalence of 38 million patients, a number that is increasing with ageing of the population (Braunwald et al. 2015). Particularly, hypertension and aortic stenosis contribute to the development of CHF (Rassa et al. 2018). In the mid-1990s, it was recognized that adverse cardiac remodeling (ACR) constitutes the pathophysiological basis leading to development of CHF (Colucci et al. 1997). Therefore, the therapeutic strategy of CHF has changed from improving myocardial contractility to preventing ACR now. ACR is usually accompanied by cardiomyocyte apoptosis and necrosis, cardiac hypertrophy, interstitial fibrosis, inflammation and vascular endothelial dysfunction (Anzai et al. 2013). Although it is not fully elucidated how hearts with pressure overload transform from compensated period to decompensated period, a mismatch between the number of myocardial capillaries and cardiomyocyte size due to insufficient cardiac angiogenesis has been reported to be mainly involved in development of CHF (Dorn et al. 2007; Higashikuni et al. 2012). Thus, promoting myocardial angiogenesis is a promising therapeutic strategy to treat CHF.

Nitric oxide (NO) plays an important role in mediating angiogenesis. It is synthesized by a family of NO synthases (NOS), including neuronal, endothelial and inducible NOS (n/e/iNOS) (Lee et al. 2016). Endothelial dysfunction in CHF patients is associated with reduced NO bioavailability (Bauersachs et al. 2004). By activating the eNOS/nNOS pathway and decreasing reactive oxygen species (ROS) production, NO bioavailability is enhanced to prevent the onset of CHF (Couto et al. 2015). On the contrary, iNOS upregulation in cardiomyocytes may accelerate cardiac dysfunction and reduce myocardial contractility in CHF (Lee et al. 2016; Shao et al. 2016).

Myocardial NO production is mainly regulated by eNOS or nNOS at early stages of CHF, whereas at late stages it is mostly deregulated and excessive released by iNOS (Massion et al. 2003). In conclusion, enhancing antioxidation and nitric oxide bioavailability is a promising method to promote angiogenesis in patients with CHF.

Ginkgolide A (GA) is a lactone extracted from *Ginkgo biloba*, a herb with long history of medical use for various, including cardio-vascular diseases (Zhaocheng et al. 2016). GA is reported to have multiple pharmacological activities such as attenuating endothelial dysfunction, reducing inflammatory response and decreasing oxidative stress *in vivo* and *in vitro* (Zhaocheng et al. 2016; Zhou et al. 2006; Li et al. 2017). So far, there no study about the effects of GA on cardiac damage in CHF mice induced by pressure overload. Thus, we aimed to detect whether GA could exhibit cardio-protective effects in mice with pressure overload through enhancing antioxidation and NO bioavailability.

2. Investigations and results

2.1. Effects of GA on heart weight/body weight ratio, heart weight/tibial length ratio and heart function in TAC mice

Among the three groups, the transverse aortic constriction (TAC) group was not treated with GA and the heart weight/body weight ratio and heart weight/tibial length ratio in this group were the highest, indicating heart hypertrophy provoked by TAC (p<0.01). Treatment with GA for four weeks significantly inhibited heart hypertrophy after TAC, as indicated by the decrease of heart weight/body weight ratio and heart weight/tibial length ratio (p<0.01) (Fig. 1A, 1B).
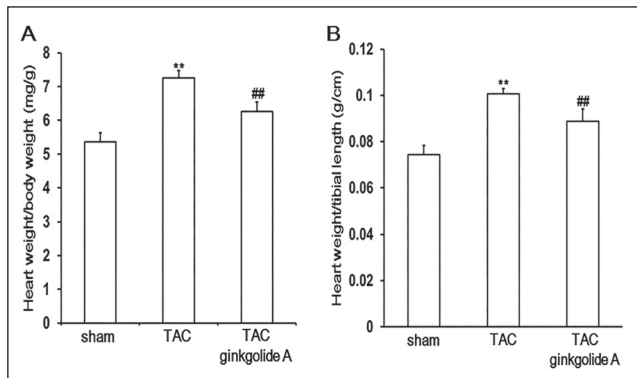
Fig. 1: Effects of GA on heart weight/body weight ratio and heart weight/tibial length ratio in TAC mice. A, B: Ratios of heart weight to body weight and tibial length. sham: n=7; TAC: n=7; ginkgolide A: n=7. GA, ginkgolide A. sham, mice with sham operation; TAC, mice with transverse aortic constriction; ginkgolide A, TAC mice with ginkgolide A treatment. Data are given as means±SEM. **$P < 0.01$ vs sham group, ##$P < 0.01$ vs TAC group.
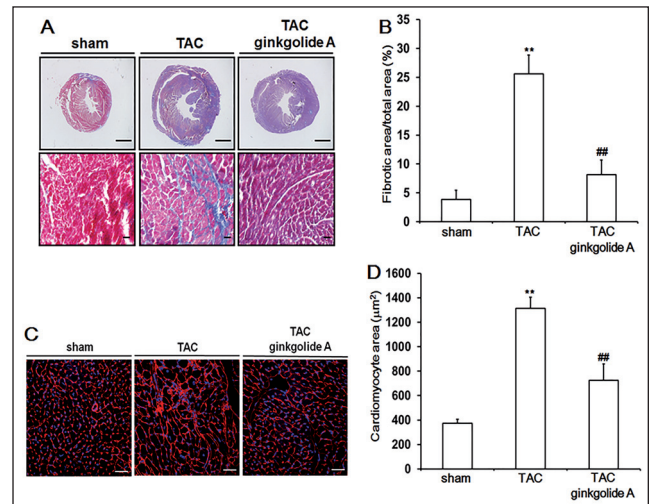

Fig. 2: Effects of GA on heart fibrotic area and cardiomyocyte hypertrophy in TAC mice. A: Masson's staining was used to display fibrotic areas (in blue). Scale bar: 1.25 mm (upper two figures). Scale bar: 40 μm (lower two figures). B: Quantitation of fibrotic area (n=3). C: WGA staining was used to display the structure and size of cardiomyocytes. Sections were from papillary muscle. Scale bar: 40 μm. D: Quantitation of cross areas of cardiomyocytes (n=3). Data are given as means±SEM. **$P < 0.01$ vs sham group, ##$P < 0.01$ vs TAC group.

Before TAC, the baseline echocardiography data among sham, TAC and TAC+GA groups were similar ($p>0.05$) (Table 1). At 4 weeks after TAC, systolic function of heart was considerably impaired, as indicated by the LVEF, LVFS and LV Vol;s measurements ($p<0.01$). Treatment with GA markedly improved cardiac systolic function four weeks after TAC ($p<0.01$) (Table 1). An increase in LV Vol;d is an index for cardiac dilation. LVIDD was highest in the TAC group, but was significantly smaller in the GA group ($p<0.01$) (Table 1). Cardiac hypertrophy and wall thickness were indicated by LV mass, LV mass corrected, IVS;d and LVPW;d. Significant heart hypertrophy and increased wall thickness were observed in TAC group, which were reversed by GA treatment ($p<0.01$) (Table 1). Taken together, these results indicated that GA attenuated cardiac hypertrophy and improved cardiac dysfunction after transverse aortic constriction (TAC) in mice.

2.2. Effects of GA on heart fibrotic area and cardiomyocyte hypertrophy in TAC mice

After surgery-induced pressure overload, fibrotic area and the size of cardiomyocytes increased notably in the left ventricle of vehicle-treated mice as compared to sham-operation mice ($p<0.01$). Four weeks after GA treatment in TAC mice, fibrotic area and cardiomyocyte size were declined significantly compared with those of the TAC group ($p<0.01$), indicating that GA reduced cardiac fibrosis and cardiomyocyte size in TAC mice (Fig. 2A, B, C, D).

2.3. Effects of GA on capillary density and cell apoptosis in TAC mice

We examined capillary density in a CD31 assay among these three groups. The results showed that capillary density decreased notably in mice of the TAC group compared with mice of the sham group ($p<0.01$). However, GA treatment substantially promoted capillary formation ($p<0.05$) (Fig. 3A, 3B). Four weeks after TAC, cell apoptosis increased notably as compared to mice with sham operation ($p<0.01$). After treatment with GA, cell apoptosis was less in GA-treated mice than that in vehicle-treated TAC mice ($p<0.01$) (Fig. 3C, D). In total, these results show that GA can promote angiogenesis and reduce cell apoptosis in hearts of TAC mice.

2.4. Effects of GA on cardiac oxidative stress and NO bioavailability in TAC mice

Increased MDA level and NOX activity, and decreased T-SOD activity in hearts confirmed that cardiac oxidative stress had been induced in TAC mice ($p<0.01$). Treatment of TAC mice with GA

Table 1: Effect of GA on heart function in TAC mice before and after TAC

Group	Before TAC			4 weeks after TAC		
	Sham	TAC	TAC+GA	Sham	TAC	TAC+GA
LV Vol;d (ml)	58.72±9.94	61.56±12.95	57.67±9.72	61.61±9.19	101.39±8.27**	76.20±6.11##
LV Vol;s (ml)	24.22±5.71	25.44±7.06	23.60±4.30	24.79±3.90	61.16±6.16**	39.75±5.78##
EF (%)	59.16±3.63	59.18±4.23	59.11±2.70	59.65±4.01	39.64±4.17**	48.04±4.32##
FS (%)	30.79±2.40	30.87±2.79	30.71±1.84	31.20±2.75	19.28±2.36**	23.94±2.56##
LV Mass	88.11±4.55	89.82±12.44	85.42±6.88	94.48±2.75	170.41±21.22**	133.57±8.68##
LV Mass Corrected	65.55±10.07	65.35±9.64	63.08±7.21	73.87±10.62	136.33±16.97**	105.14±9.00##
IVS;d (mm)	0.64±0.07	0.67±0.06	0.62±0.06	0.72±0.05	1.04±0.07**	0.85±0.08##
LVPW;d (mm)	0.62±0.05	0.64±0.04	0.63±0.05	0.72±0.08	0.91±0.09**	0.77±0.11##

GA: ginkgolide A; LV Vol;d: left ventricular end diastolic volume; LV Vol;s: left ventricular end systolic volume; EF: eject fraction; FS: fractional shortening; IVS;d: diastolic interventricular septum; LVPW;d: diastolic left ventricular posterior wall. Data are given as means±SEM. **$P < 0.01$ vs sham group, #$P < 0.05$, ##$P < 0.01$ vs TAC group.
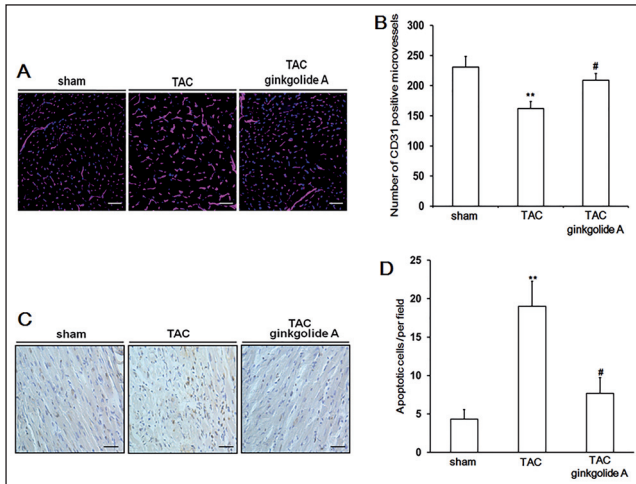
Fig. 3: Effects of GA on capillary density and cell apoptosis in TAC mice. A: CD31 staining was used to show capillary density. Scale bar: 40 μm. D: Quantitation of capillary density (n=3). C: TUNEL staining was used to show cell apoptosis. Brown yellow in cell nucleus indicated apoptotic cell. Scale bar: 40 μm. B, Quantitation of apoptotic cell number (n=3). Data are given as means±SEM. **$P < 0.01$ vs sham group, #$P < 0.05$, ##$P < 0.01$ vs TAC group.
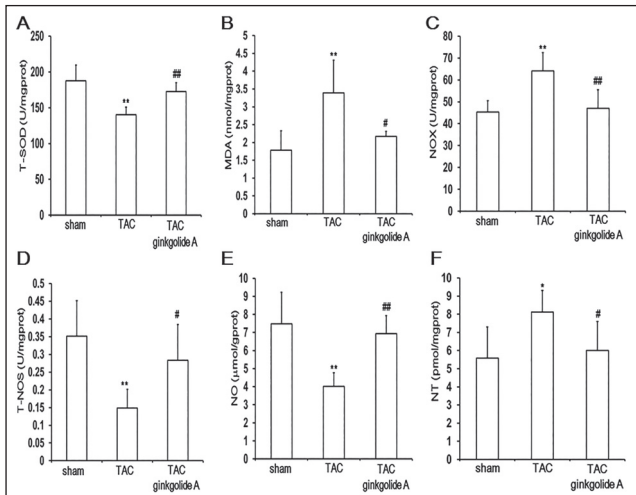

Fig. 4: Effects of GA on cardiac oxidative stress and NO bioavailability in TAC mice. A-C: Effect of GA on cardiac oxidative stress as indicative of activities of T-SOD and NOX, and MDA level. D-F: Effect of GA on NO bioavailability indicated by T-NOS activity and levels of NT and NO. NO, nitric oxide; T-SOD, total-superoxide dismutase; MDA, malonaldehyde; NOX, NAPDH oxidase; T-NOS, total NO synthases; NT, nitrotyrosine. sham: n=7; TAC: n=7; ginkgolide A: n=7. Data are given as means±SEM. *$P < 0.05$, **$P < 0.01$ vs sham group, #$P < 0.05$, ##$P < 0.01$ vs TAC group.

reduced MDA level and NOX activity, and increased T-SOD activity, suggesting that GA had anti-oxidative activity in hearts of TAC mice ($p<0.05$, $p<0.01$) (Fig. 4A, B, C).

After TAC surgery, T-NOS activity and NO level in hearts were reduced significantly, and NT levels were augmented notably, indicating that low NO bioavailability occurred in hearts of mice with pressure overload ($p<0.05$, $p<0.01$). When TAC mice had been treated with GA for four weeks, T-NOS activity and NO level in hearts were increased and NT level was decreased markedly, suggesting that GA enhanced cardiac NO bioavailability in mice with pressure overload ($p<0.05$, $p<0.01$) (Fig. 4D, E, F).

2.5. Effects of GA on expressions of TGF-β and NOS family in the hearts of TAC mice

To further investigate the possible molecular mechanism by which GA promoted cardiac angiogenesis and improved cardiac remodeling, we examined protein expressions of TGF-β and NOS family
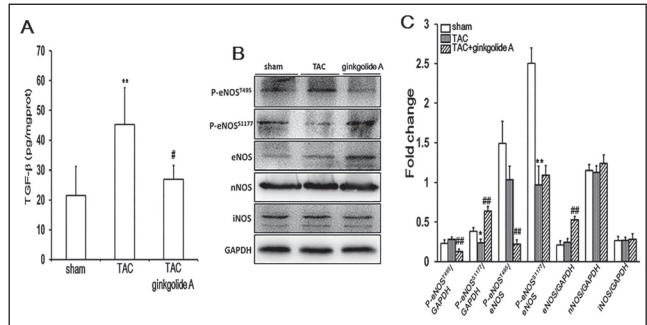

Fig. 5: Effects of GA on protein expressions of TGF-β and NOS family in the hearts of TAC mice. A: Effect of GA on TGF-β expression in hearts of TAC mice. sham: n=7; TAC: n=7; ginkgolide A: n=7. B: Effect of GA on NOS family expression including n/e/iNOS in hearts of TAC mice. C: Quantitative study (n=3). Data are given as means±SEM. *$P < 0.05$ vs sham group, ##$P < 0.01$ vs TAC group.

in heart. After TAC for four weeks, there were no significant differences about, phosphorylation of eNOS Thr 495 and expressions of eNOS, nNOS and iNOS between the hearts of TAC mice and those in sham-operation mice ($p>0.05$). However, phosphorylation of eNOS Ser 1177 were increased significantly and TGF-β levels were increased markedly in the hearts of TAC mice as compared to sham mice ($p<0.05$, $p<0.01$).

GA administration can significantly increase eNOS expression and the phosphorylation of eNOS Ser 1177 in the hearts of mice with TAC ($p<0.01$). Meanwhile, cardiac TGF-β level and the phosphorylation of eNOS Thr 495 in GA-treated mice declined markedly as compared to mice of the TAC group ($p<0.05$, $p<0.01$). However, chronic GA medication had no effect on protein expressions of nNOS and iNOS in myocardium of TAC mice ($p>0.05$). (Fig. 5A, B, C). In conclusion, chronic GA treatment can reduce TGF-β level and increase eNOS activity in the hearts of TAC mice.

2.6. Effects of GA on BW, heart weight/tibial length ratio, heart function and histology in normal mice

At last, we tested whether only GA treatment had any effect on body weight (BW), heart weight/tibial length ratio, cardiac function and histology for four weeks. After treatment of normal mice with GA for four weeks, there were no significances in BW, heart weight/tibial length ratio and heart function between PBS group and GA group ($p>0.05$) (Table 2). From HE staining, the cardiac histology of PBS group was not changed as compared to GA group (Fig. 6). Totally, these data suggested that the dose of GA had no disadvantage in hearts of normal mice.

3. Discussion

Ginkgo biloba has been used as a traditional medicine for a long time, especially against cardiovascular diseases, but the underlying mechanisms are not yet elucidated. It has been reported that gink-

Table 2: Effect of GA on BW, BW/TL and heart function in normal mice

	Control group (n=7)	GA group (n=7)
BW (g)	24.05±1.00	23.93±1.27
BW/TL (g/cm)	0.076±0.004	0.075±0.004
LV Vol;d (ml)	62.96±12.50	60.44±14.28
LV Vol;s (ml)	27.42±7.02	25.80±7.18
EF (%)	56.89±3.43	57.68±2.57
FS (%)	29.31±2.15	29.77±1.60
LV Mass	89.31±11.26	88.44±11.70
LV Mass Corrected	72.31±9.99	71.04±9.37

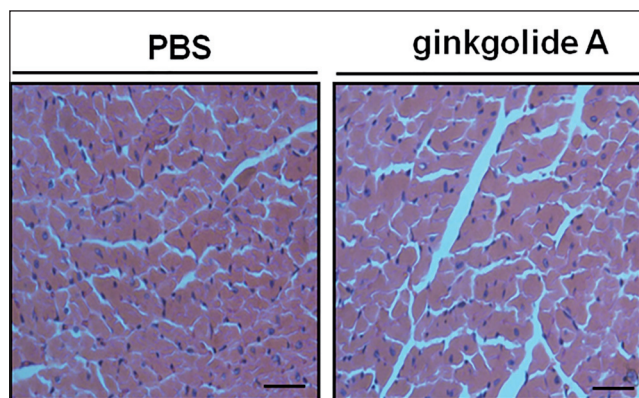BW: body weight; TL: tibial length. Data are given as means±SEM.

Fig. 6: Effects of GA on cardiac histology by HE in normal mice. HE: hematoxylin-eosin staining. Scale bar: 40 μm.

golide A (GA), one of the major constituents of *Ginkgo biloba*, can protect against homocysteine-induced endothelial damage through reducing oxidative stress and upregulation of eNOS messenger RNA and protein levels in porcine coronary arteries (Zhou et al. 2006). However, there is report on the effects of GA on heart damage in CHF mice induced by pressure overload through enhancing antioxidation and NO utilization. In the present study, we found that GA rendered cardio-protection against ACR in mice with pressure overload, the mechanism of which was associated with its anti-oxidative ability to reduce NO consumption and with enhancing eNOS activity to increase NO production.

Oxidative stress is the status that the cell is under redox imbalance, which means that ROS levels exceed the scavenging capacity of the antioxidative defense system (such as T-SOD) (Braunwald et al. 2017). ROS affect almost every aspect of ACR, including hypertrophic response, endothelial dysfunction and extracellular matrix deposition (Lassegue et al. 2012). ROS can take effect on polyunsaturated fatty acid, leading to disturbance of cell's membrane lipid bilayer arrangement and formation of unsaturated aldehyde (MDA). These metabolites can inactivate many cellular proteins to cause cytotoxicity by formatting protein cross-linkages (Esterbauer et al. 1986). In our study, low-activity T-SOD and high-level MDA were indicative of oxidative stress in the heart of mice with pressure overload. GA treatment can enhance T-SOD activity and reduce MDA level in the heart, suggesting that GA had antioxidative ability. The result was similar to those of a previous study from (Zhou et al. 2006). The upregulated TGF-β expression is a locally secreted cytokine that has been implicated as a major contributor to cardiac hypertrophy and fibrosis in humans and experimental models, which can be partly triggered by oxidative stress (Liu et al. 2018). Cardiac TGF-β overexpression of TAC mice was found in our study, which was inhibited by GA treatment, suggesting that antioxidation of GA was closely associated with low TGF-β expression in hearts of TAC mice. It is reported that GA can block superoxide anion production in homocysteine-stimulated porcine coronary arteries and nutrition-deprived vascular smooth muscle cells (Zhou et al. 2006; Weakley et al. 2011). NOX are the main sources of ROS in the cardiovascular system, with increased activity in hearts under pressure overload (Lassegue et al. 2012; Bedard et al. 2007). From our study, we can conclude that the antioxidative effect of GA was attributed to cardiac NOX activity inhibition after TAC induction.

Under the condition of oxidative stress, NO can easily react with O^{2-} to form peroxynitrite ($ONOO^-$), which nitrates tyrosine residues in proteins to form a stable metabolite, 3-nitrotyrosine (NT, Wanyong et al. 2015). In the present study, increased NT level and reduced NO level were observed in hearts of mice with pressure overload, indicating that NO modulation was weakened due to excessive ROS generation. Cardiac NO bioavailability was enhanced as a result of antioxidative effect of GA in TAC mice. NO is synthesized from its precursor l-arginine by a family member of NOS (nNOS, iNOS or eNOS) (Lee et al. 2016). Increased NO utilization can prevent

the development of CHF through enhancing eNOS/nNOS pathway activation. Ser1177 and Thr 495 are two phosphorylation sites which can regulate eNOS activity. Phosphorylation at Ser1177 activates eNOS, whereas phosphorylation at Thr 495 inactivates eNOS (Ruetten et al. 2005; Niu et al. 2012). iNOS over-expression is detrimental to CHF development, which can be reversed by genetic and pharmacologic iNOS inhibition (Zhang et al. 2007). In the study, we found that cardiac T-NOS activity was significantly low in TAC mice, and there were no differences in protein expressions of eNOS, nNOS and iNOS between sham and TAC groups. However, TAC can markedly inhibit phosphorylation of eNOS Ser 1177 in the heart of mice, implying that reduced eNOS activity mainly contributed to low T-NOS activity in heart of mice with pressure overload. GA can upregulate eNOS mRNA and protein expressions and increase NO level in homocysteine-stimulated porcine coronary arteries and porcine coronary artery endothelial cells (Zhou et al. 2006). After TAC mice had been treated with GA for four weeks, T-NOS activity, eNOS protein expression and phosphorylation of eNOS Ser 1177 were obviously increased in hearts of TAC mice except for no changes of nNOS and iNOS protein expressions, but phosphorylation of eNOS Thr 495 was notably declined, indicating that GA enhanced NO bioavailability mainly through strengthening eNOS activity in mice with pressure overload.

In conclusion, GA had a cardioprotective effect in mice with pressure overload, which was closely related with reducing ROS generation and enhancing NO bioavailability in hearts.

4. Experimental

4.1. Mice, transverse aortic constriction (TAC) model and GA treatment

Male mice at the age of 8 weeks from C57BL/6 background were housed in groups with 12 h dark-light cycles and free access to food and water. These conditions were in accordance with the Guide for the Care and Use of Laboratory Animals published by the US National Institutes of Health (NIH publication no. 85-23, revised in 1996), and the regulations on mouse welfare and ethics of Nanjing University. The animal protocol was reviewed and approved by the Ethics Committee of Model Animal Research Center of Nanjing University.

TAC in mice was generated following a method previously reported with slight modifications. Briefly, mice were anaesthetized intraperitoneally with pentobarbital sodium (30-50 mg/kg). Before TAC, we measured the aortic arch diameter by echocardiography. Furthermore, TAC procedure was only done by an experienced operator. An endotracheal tube was introduced, and a volume-cycled rodent respirator (model 683; Harvard Apparatus, Holliston, MA) provided positive pressure ventilation at 2 to 3 mL per cycle with a respiratory rate of 120 cycles per minute. After the left parasternal skin incision, the transverse aorta was exposed between the thymus gland, and a 7-0 silk suture was placed around a 27-gauge blunt-ended needle on the transverse aorta, which was removed immediately to yield a narrowing 0.4 mm in diameter. Sham-operation was performed in mice using the same procedure without the transverse aortic ligation. The chest wound was closed with a 7-0 silk suture (Niu et al. 2012).

Ginkgolide A (GA, purity 98%, molecular formula. $C_{20}H_{24}O_9$, molecular weight. 408.4, Cas No. 15291-75-5, Nanjing DASF Bio-Technology Co., Ltd., Nanjing, China) was dissolved in phosphate buffer solution (PBS). Twenty-one mice were randomly assigned into three groups as follows: sham-operation group (without TAC and only received an intraperitoneal injection of 10 ml/kg/day PBS, n=7), TAC group (TAC and received an intraperitoneal injection of 10 ml/kg/day PBS, n=7) and GA-treated group (TAC and received an intraperitoneal injection of GA at the dose of 20 mg/kg/day, n=7) (Li et al. 2017). Additionally, there were no significances in aortic arch diameter and stenosis degree between TAC group and GA-treated group before and after TAC, respectively (Fig. 7). Mice in all groups were treated for 4 weeks.
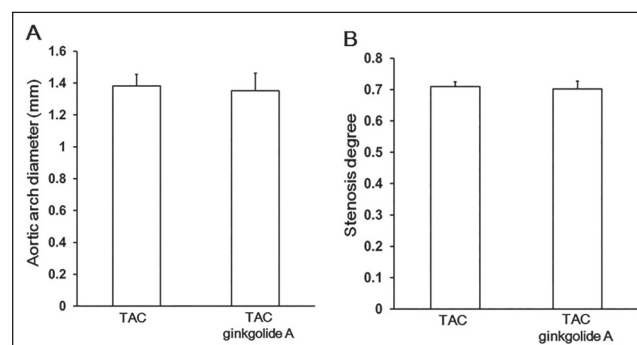

Fig. 7: Effects of GA on aortic arch diameter and stenosis degree between TAC group and GA group before and after TAC. TAC: n=7; ginkgolide A: n=7. Data are given as means±SEM.

4.2. Cardiac function assessment by echocardiography

On day 28 following TAC induction, an echocardiographic examination was performed using a Vevo 770 UBM system (Visual Sonics, Toronto, Canada), equipped with a 30-MHz transducer, which was used for noninvasive transthoracic echocardiography. Two-dimensional guided M-mode tracings were recorded. The internal diameter of the LV in the short-axis plane was measured at end diastole and end systole from M-mode recordings just below the tips of the mitral valve leaflets. After measurement, left ventricular end diastolic volume (LV Vol;d) as indicative of heart diastolic function were determined. Three indexes of heart systolic function including left ventricular end systolic volume (LV Vol;s), LV fractional shortening (LVFS) and LV ejection fraction (LVEF) were calculated. LV mass and LV mass corrected were two indexes of cardiac hypertrophy. Diastolic interventricular septum (IVS;d) and diastolic left ventricular posterior wall (LVPW;d) were shown to exhibit heart wall thickness (You et al. 2018).

4.3. Spectrophotometry determination and enzyme linked immunosorbent assay (ELISA)

Total-superoxide dismutase (T-SOD), malonaldehyde (MDA), nicotinamide adenine dinucleotide phosphate (NAPDH) oxidase (NOX), total NOS (T-NOS) and NO analysis kits were all purchased from Jiancheng Bioengineering Institute (Nanjing, China). ELISA test boxes for nitrotyrosine (NT) and transforming growth factor-β (TGF-β) were provided by Meimian Biotechnology Co., Ltd. (Wuhan, China) and Beijing 4A Biotech Co., Ltd. (Beijing, China), respectively. The levels of T-SOD, MDA, NOX, T-NOS and NO of heart homogenate were determined by Visible spectrophotometer (Puxi Tongyong Instrument Co., Ltd., Beijing, China). Contents of NT and TGF-β were determined by Microplate reader (Bio Tek Co., Ltd., America). Samples were handled according to manufacturers' instructions before measured.

4.4. Western blot analysis

Western blot analyses were performed as previously reported (Li et al. 2017). Left ventricles of mice were dissected and snap-frozen in liquid nitrogen. Tissue lysates were prepared in lysis buffer (20 mM Tris, 150 mM NaCl, 10% glycerol, 20 mM glycerophosphate, 1% NP40, 5 mM ethylenediaminetetraacetic acid (EDTA), 0.5 mM ethylenebis (oxyethylenenitrilo) tetraacetic acid (EGTA), 1 mM Na3VO4, 0.5 mM phenylmethanesulfonyl fluoride (PMSF), 1 mM benzamidine, 1 mM dl-dithiothreitol (DTT), 50 mM NaF, 4 mM leupeptin, pH=8.0). Equal amounts of total proteins (50 mg) were resolved by 10% sodium dodecyl sulfate-polyacrylamide gel electrophoresis (SDS-PAGE) and transferred to polyvinylidene fluoride (PVDF) membranes (Millipore, Billerica, MA, USA). Membranes were blocked with 5% non-fat milk in Tris Buffered saline (TBST) (50 mM Tris, 150 mM NaCl, 0.5 mM Tween-20, pH=7.5) and then incubated overnight with primary antibodies. Phospho-eNOS (Ser1177), phospho-eNOS (Thr 495), eNOS, nNOS and iNOS were produced from ABclonal Technology. GAPDH and HRP-linked secondary antibodies were purchased from Bioworld Technology and Thermos Scientific, respectively. Image J software (NIH) was used to perform densitometric analysis.

4.5. Histology, immunofluorescence staining and immunochemistry

The protocols for Masson's staining, hematoxylin-eosin staining (HE) and immunefluorescence (IF) were performed as reported previously (You et al. 2018). Briefly, heart samples were first washed with ice-cold PBS and then fixed in 4% paraformaldehyde at 4 °C. The samples were processed successively by (a) a 30 min washing in PBS at 4 °C; (b) 15 min each in 30, 50, 75, and 85% ethanol, and then incubated for 2×10 min in 95 and 100% ethanol at room temperature (RT); (c) 3×10 min of incubation in xylene at RT; (d) 20 min of incubation in paraffin/xylene (1:1) at 65°C; and (e) 3×30 min of incubation in fresh paraffin at 65 °C. The processed heart samples were embedded in paraffin and sliced into a thickness of 6 mm, and then the sections were stained for Masson and HE.

IF staining was performed by using anti-wheat germ agglutinin (WGA) (Abcam) and anti-CD31 (BD bioscience) antibodies at 4 °C room overnight. Goat anti-rabbit IgG (Abcam) and goat anti-rat IgG (Invitrogen) diluted in PBS was then incubated for 2 h at room temperature. Fluorescence microscopy images were obtained with a Research Fluorescence Microscope (Olympus America Inc., Center Valley, PA, USA) equipped with a digital camera. Images were collected and recorded by using Adobe PhotoshopR 5.0 (Adobe Systems Inc., San Jose, CA, USA) on an IBM R52 computer (IBM, Armonk, NY, USA).

Apoptosis was assessed by Terminal-deoxynucleoitidyl Transferase Mediated Nick End Labeling (TUNEL) assay using an in situ cell death detection kit (Roche Applied Science). Fibrotic area, cardiomyocyte area, capillary number and apoptotic cells were measured with 400×magnification, and averaged after calculating in 5 high-power fields.

4.6. Statistical analysis

Data are presented as mean±SEM values. Statistical analyses were performed using SPSS version 20 (SPSS Inc., Chicago, Illinois, USA). Tukey's post-hoc test was used between two groups following a $p<0.05$ of one-way ANOVA. A $p<0.05$ was considered statistically significant.

References

Anzai T (2013) Post-infarction inflammation and left ventricular remodeling: a double-edged sword. Circ J 77: 580-587.

Bauersachs J, Schafer A (2004) Endothelial dysfunction in heart failure: mechanisms and therapeutic approaches. Curr Vasc Pharmacol 2: 115-124.

Bedard K, Krause KH (2007) The NOX family of ROS-generating NADPH oxidases: physiology and pathophysiology. Physiol Rev 87: 245-313.

Braunwald E (2015) The war against heart failure: the Lancet lecture. Lancet 385: 812-824.

Cervantes Gracia K, Llanas-Cornejo D, Husi H (2017) CVD and oxidative stress. J Clin Med 6: pii E22.

Colucci WS (1997) Molecular and cellular mechanisms of myocardial failure. Am J Cardiol 80: 15L-25L.

Couto GK, Britto LR, Mill JG, Rossoni LV (2015) Enhanced nitric oxide bioavailability in coronary arteries prevents the onset of heart failure in rats with myocardial infarction. J Mol Cell Cardiol 86: 110-120.

Dorn GW (2007) Myocardial angiogenesis: its absence makes the growing heart founder. Cell Metab 5: 326-327.

Esterbauer H, Koller E, Slee RG, Koster JF (1986) Possible involvement of the lipid-peroxidation product 4-hydroxynonenal in the formation of fluorescent chromolipids. Biochem J 239: 405-409.

Higashikuni Y, Sainz J, Nakamura K, Takaoka M, Enomoto S, Iwata H, Tanaka K, Sahara M, Hirata Y, Nagai R, Sata M (2012) The ATP-binding cassette transporter ABCG2 protects against pressure overload-induced cardiac hypertrophy and heart failure by promoting angiogenesis and antioxidant response. Arterioscler Thromb Vasc Biol 32: 654-661.

Lassegue B, San Martin A, Griendling KK (2012) Biochemistry, physiology, and pathophysiology of NADPH oxidases in the cardiovascular system. Circ Res 110: 1364-1390.

Lee J, Bae EH, Ma SK, Kim SW (2016) Altered nitric oxide system in cardiovascular and renal diseases. Chonnam Med J 52: 81-90.

Li Y, Wu Y, Yao X, Hao F, Yu C, Bao Y, Wu Y, Song Z, Sun Y, Zheng L, Wang G, Huang Y, Sun L, Li Y (2017) Ginkgolide A ameliorates LPS-induced inflammatory responses in vitro and in vivo. Int J Mol Sci 18: pii: E794.

Liu X, Tong Z, Chen K, Hu X, Jin H, Hou M (2018) The Role of miRNA-132 against apoptosis and oxidative stress in heart failure. Biomed Res Int 2018: 3452748.

Massion PB, Feron O, Dessy C, Balligand JL (2003) Nitric oxide and cardiac function: ten years after, and continuing. Circ Res 93: 388-398.

Niu X, Watts VL, Cingolani OH, Sivakumaran V, Leyton-Mange JS, Ellis CL, Miller KL, Vandegaer K, Bedja D, Gabrielson KL, Paolocci N, Kass DA, Barouch LA (2012) Cardioprotective effect of beta-3 adrenergic receptor agonism: role of neuronal nitric oxide synthase. J Am Coll Cardiol 59: 1979-1987.

Rassa A, Zahr F (2018) Hypertension and aortic stenosis: a review. Curr Hypertens Rev 14: 6-14.

Ruetten H, Dimmeler S, Gehring D, Ihling C, Zeiher AM (2005) Concentric left ventricular remodeling in endothelial nitric oxide synthase knockout mice by chronic pressure overload. Cardiovasc Res 66: 444-453.

Shao Q, Cheng HJ, Callahan MF, Kitzman DW, Li WM, Cheng CP (2016) Overexpression myocardial inducible nitric oxide synthase exacerbates cardiac dysfunction and beta-adrenergic desensitization in experimental hypothyroidism. Int J Cardiol 204: 229-241.

Weakley SM, Wang X, Mu H, Lu J, Lin PH, Yao Q, Chen C (2011) Ginkgolide A-gold nanoparticles inhibit vascular smooth muscle proliferation and migration in vitro and reduce neointimal hyperplasia in a mouse model. J Surg Res 171, 31-39.

Wanyong Y, Zefeng T, Xiufeng X, Dawei D, Xiaoyan L, Ying Z, Yaogao F (2015) Tempol alleviates intracerebral hemorrhage-induced brain injury possibly by attenuating nitrative stress. Neuroreport 26: 842-849.

You W, Wu Z, Ye F, Wu X (2018) Cardamonin protects against adverse cardiac remodeling through mTORC1 inhibition in mice with myocardial infarction. Pharmazie 73: 508-512.

Zhaocheng J, Jinfeng L, Luchang Y, Yequan S, Feng L, Kai W (2016) Ginkgolide A inhibits lipopolysaccharide-induced inflammatory response in human coronary artery endothelial cells via downregulation of TLR4-NF-kappaB signaling through PI3K/Akt pathway. Pharmazie 71: 588-591.

Zhang P, Xu X, Hu X, van Deel ED, Zhu G, Chen Y (2007) Inducible nitric oxide synthase deficiency protects the heart from systolic overload-induced ventricular hypertrophy and congestive heart failure. Circ Res 100: 1089-1098.

Zhou W, Chai H, Courson A, Lin PH, Lumsden AB, Yao Q, Chen C (2006) Ginkgolide A attenuates homocysteine-induced endothelial dysfunction in porcine coronary arteries. J Vasc Surg; 44: 853-862.